Dispersive Decay for the Free Schrödinger Equation and a Higher-Order Model

Rakhim Baimurzin

Department of Mathematics, Nazarbayev University

Supervisor: Adilbek Kairzhan

Second Reader: Tesfahun Achenef

Abstract

This undergraduate capstone project studies the pointwise decay of solutions to two dispersive equations: the free Schrödinger equation $iu_t = u_{xx}$ and the third-order model $iu_t = u_{xx} - iu_{xxx}$. Under suitable regularity assumptions on the initial data, we prove the estimates $\|u(\cdot, t)\|_{L^\infty} \lesssim t^{-1/2}$ and $\|u(\cdot, t)\|_{L^\infty} \lesssim t^{-1/3}$ respectively, via explicit Fourier analysis and a cutoff argument in frequency space. The numerical simulations confirm these rates and compare the theoretical bounds to the observed decay.

Contents

1 Introduction

1.1 Decay and dispersion

The study of decay for solutions to PDEs is a natural and recurring question. A helpful first intuition comes from physical wave phenomena: a pebble dropped into still water creates a splash that gradually spreads outward, the ripples flattening as they travel. Many PDEs exhibit the same qualitative behavior — solutions that begin concentrated tend to spread across the domain and decay in amplitude over time.

We are interested in making this precise by estimating $\|u(\cdot,t)\|_{L^\infty}$, the supremum of the solution at time t. Such a bound is a fundamental characteristic of the equation: it rules out sudden large concentrations and gives a quantitative rate at which the solution flattens. Beyond this, knowing the decay rate is useful for further analysis — particularly when the solution is expressed in a form that involves an integral over time. In such cases the decay of the integrand directly controls the size of the integral. One concrete example is Duhamel's formula for a nonlinear Schrödinger equation,

$$u(t) = e^{it\partial_{xx}}u_0 + \int_0^t e^{i(t-s)\partial_{xx}}\left(|u|^2u\right)ds,$$

where a bound $\|e^{it\partial_{xx}}f\|_{L^\infty} \leq Ct^{-1/2}\|f\|_X$ makes the integral term controllable for small initial data, yielding global existence; see for instance [2] for a concrete instance of this program.

1.2 Outline

Section 2 sets up the necessary definitions: L^p norms, the Fourier transform, and the phase function. Section 3 treats the free Schrödinger equation $iu_t = u_{xx}$, proving the $t^{-1/2}$ decay estimate by two methods. Section 4 handles the third-order model $iu_t = u_{xx} - iu_{xxx}$, proving the $t^{-1/3}$ rate in the no-stationary-point regime. Section 5 presents numerical simulations confirming both rates.

1.3 Visualisation

A numerical simulation of the free Schrödinger equation and the higher-order model over time is presented in Section 5. Figure 1 shows three snapshots of the free Schrödinger solution with Gaussian initial data, illustrating the dispersive spreading. The red curve is the modulus $|u|$, orange is $\mathrm{Re}(u)$, and purple is $\mathrm{Im}(u)$.

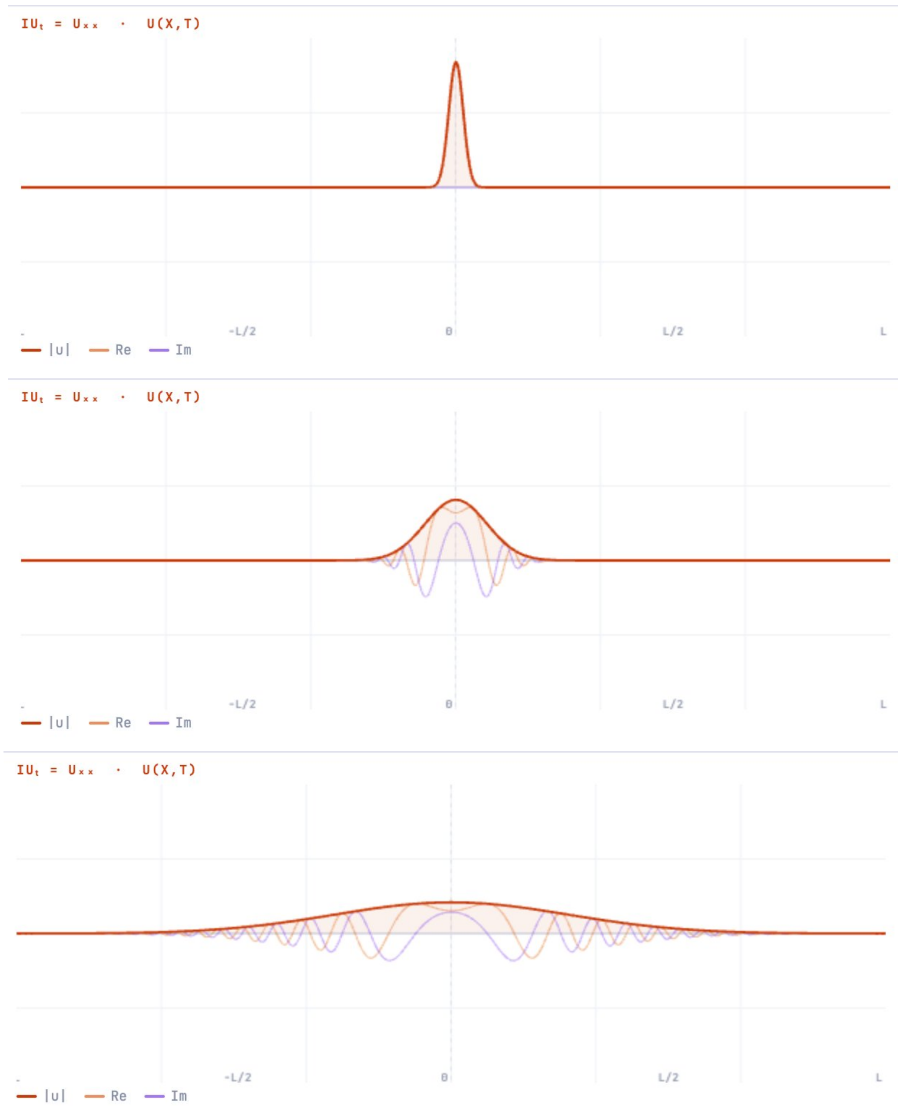

Figure 1: Free Schrödinger equation $iu_t = u_{xx}$ with Gaussian initial data at times $t = 0$, $t = 2$, $t = 8$. Suprema: $\|u\|_{L^\infty} = 1,\ 0.4846,\ 0.2491$, consistent with $t^{-1/2}$ decay.

2 Preliminaries

2.1 L^p spaces and norms

Let $f : \mathbb{R} \to \mathbb{C}$ be a measurable function. For $1 \le p < \infty$ we define the L^p norm by

$$\|f\|_{L^p(\mathbb{R})} = \left(\int_{\mathbb{R}} |f(x)|^p \, dx \right)^{1/p},$$

and the L^∞ norm by

$$\|f\|_{L^\infty(\mathbb{R})} = \operatorname{ess\,sup}_{x\in\mathbb{R}} |f(x)| \, .$$

We say $f \in L^p(\mathbb{R})$ if $\|f\|_{L^p} < \infty$. The three spaces most relevant to this paper are:

- $L^1(\mathbb{R})$: functions with finite total integral $\int_{\mathbb{R}} |f(x)| \, dx < \infty$. These are absolutely integrable functions.

- $L^2(\mathbb{R})$: functions with finite energy $\int_{\mathbb{R}} |f(x)|^2\,dx < \infty$. This is the natural space for wave equations, as $\|f\|_{L^2}^2$ represents the total energy (or mass) of the wave.
- $L^\infty(\mathbb{R})$: functions that are essentially bounded. The norm $\|f\|_{L^\infty}$ captures the supremum of $|f|$, i.e. the largest pointwise amplitude.

Decay of a solution $u(x,t)$ is measured in L^∞ because we are asking how large the solution can be at any single point in space. A bound $\|u(\cdot,t)\|_{L^\infty} \le Ct^{-\alpha}$ says the pointwise amplitude shrinks at rate $t^{-\alpha}$, regardless of where in space we look. The L^2 norm, by contrast, is conserved for both equations we study — so L^∞ is the right norm to capture the spreading and flattening of the wave.

We write $A \lesssim B$ to mean $A \le CB$ for some constant $C > 0$ independent of t.

2.2 Fourier transform

We work throughout on the real line $\mathbb{R}$. The Fourier transform and its inverse are normalised symmetrically:

$$\widehat{f}(k) = \frac{1}{\sqrt{2\pi}} \int_{\mathbb{R}} f(x)\,e^{-ikx}\,dx, \qquad f(x) = \frac{1}{\sqrt{2\pi}} \int_{\mathbb{R}} \widehat{f}(k)\,e^{ikx}\,dk. \tag{1}$$

The variable k is the frequency (or wavenumber). With this normalisation, Plancherel's theorem states that the Fourier transform is an isometry on L^2:

$$\|f\|_{L^2(\mathbb{R})} = \left\|\widehat{f}\right\|_{L^2(\mathbb{R})}.$$

This is the precise sense in which L^2 energy is conserved when passing to frequency space. We use the standard differentiation rule $\widehat{\partial_x^n f}(k) = (ik)^n \widehat{f}(k)$, which converts differential operators into multiplication by powers of ik, and the differentiation-in-frequency identity

$$\partial_k \widehat{f}(k) = -\frac{i}{\sqrt{2\pi}} \int_{\mathbb{R}} x\,f(x)\,e^{-ikx}\,dx, \tag{2}$$

showing that differentiating in frequency corresponds to multiplication by x in physical space. In the cutoff estimates below we assume directly that $\partial_k \widehat{f} \in L^1$.

2.3 Phase function

When a PDE is solved via the Fourier transform, the solution typically takes the form

$$u(x,t) = \frac{1}{\sqrt{2\pi}} \int_{\mathbb{R}} e^{-it\Phi(k)} \widehat{u_0}(k)\,dk,$$

where $\Phi : \mathbb{R} \to \mathbb{R}$ is called the *phase function*. It encodes the dispersion relation of the equation: different frequencies k travel at different speeds determined by Φ. The decay of u in L^∞ is governed entirely by the oscillatory behavior of $e^{-it\Phi(k)}$ for large t, and specifically by the geometry of Φ'. Points where $\Phi'(k) = 0$ are called *stationary points*; near these the oscillation is slowest and the dominant contribution to the integral is concentrated. The rate at which $|\Phi'|$ vanishes at its minimum determines the decay rate, as we will see concretely in Sections 3 and 4. The material in this section follows [1].

2.4 Energy conservation

For both equations studied in this paper, the L^2 norm of the solution is conserved: $\|u(\cdot,t)\|_{L^2} = \|u_0\|_{L^2}$ for all t. This follows from Plancherel's theorem and the fact that the Fourier multiplier $e^{it\lambda(k)}$ has modulus one for real $\lambda(k)$. The physical meaning is that the total energy of the wave does not dissipate — under perfect conditions the wave does not disappear, it simply spreads out indefinitely. The L^∞ decay we prove is therefore not a loss of energy but a consequence of this spreading: the same fixed energy is distributed over an ever-growing region, forcing the pointwise amplitude to zero.

2.5 Motivation for the higher-order model

Consider the general linear dispersive equation with constant coefficients up to third order:

$$iu_t = ai\,u_{xxx} + b\,u_{xx} + ci\,u_x + d\,u.$$

Taking the Fourier transform, the right-hand side contributes a phase $\omega(k) = -ak^3 - bk^2 + ck + d$ to the dispersion relation. The constant term d contributes only a global phase factor e^{-idt} of modulus one and has no effect on decay. The linear term ck shifts the group velocity uniformly — in physical terms it merely translates the solution at constant speed without causing any spreading — so it too is irrelevant to decay and can be dropped. We are thus left with

$$iu_t = ai\,u_{xxx} + b\,u_{xx}.$$

If $b \neq 0$, we may divide through by b and relabel to obtain $iu_t = \alpha\, iu_{xxx} + u_{xx}$. Setting $\alpha = -1$ for concreteness gives the model

$$iu_t = u_{xx} - iu_{xxx},$$

which is the equation studied in Section 4.

3 The Free Schrödinger Equation

3.1 Problem statement and assumptions

We study the Cauchy problem for the free Schrödinger equation

$$iu_t = u_{xx}, \qquad u(x,0) = u_0(x), \qquad x \in \mathbb{R},\ t > 0. \tag{3}$$

We impose the following assumptions on the initial data:

$$\widehat{u_0} \in L^\infty(\mathbb{R}), \qquad \partial_k \widehat{u_0} \in L^1(\mathbb{R}). \tag{4}$$

The first two conditions say that the Fourier transform of the initial data is absolutely integrable and bounded; the third says it has some regularity in frequency space. Under these assumptions we will prove:

Proposition 3.1. *Let u be the solution of* (3) *with initial data satisfying* (4)*. Then for all $t > 0$,*

$$|u(x,t)| \lesssim t^{-1/2}\big(\|\widehat{u_0}\|_{L^\infty} + \|\partial_k \widehat{u_0}\|_{L^1}\big).$$

The bound is uniform in x and shows that the L^∞ norm of the solution decays at rate $t^{-1/2}$. Note that the L^2 norm is conserved (see below), so the decay is purely a spreading effect: the same total energy is distributed over an ever-larger region, forcing the pointwise amplitude to decrease.

3.2 Fourier-space representation and L^2-conservation

Applying the Fourier transform in x to (3), using $\widehat{u_{xx}} = -k^2 \widehat{u}$, gives the ODE

$$\partial_t \widehat{u}(k,t) = ik^2 \widehat{u}(k,t),$$

which is solved immediately by $\widehat{u}(k,t) = e^{itk^2}\widehat{u_0}(k)$. Inverting via (1):

$$u(x,t) = \frac{1}{\sqrt{2\pi}} \int_{\mathbb{R}} e^{i(xk+tk^2)} \widehat{u_0}(k)\, dk. \tag{5}$$

Since $\left|e^{itk^2}\right| = 1$, Plancherel's theorem gives immediately $\|u(\cdot,t)\|_{L^2} = \|u_0\|_{L^2}$.

The solution is now expressed as an oscillatory integral with phase $\Phi(k) = -xk/t - k^2$ (after factoring out t). All decay information is encoded in the behavior of this integral for large t.

3.3 Method 1: Kernel computation by completing the square

For the Schrödinger equation the phase is exactly quadratic, which allows us to identify the integral kernel explicitly. Completing the square in (5) gives

$$xk + tk^2 = t\Big(k + \frac{x}{2t}\Big)^2 - \frac{x^2}{4t}.$$

Equivalently, for sufficiently regular initial data one obtains the standard kernel representation

$$u(x,t) = \frac{e^{i\pi/4}}{\sqrt{4\pi t}} \int_{\mathbb{R}} e^{-i(x-y)^2/(4t)} u_0(y)\, dy, \qquad t > 0. \tag{6}$$

The oscillatory factor has modulus one. Therefore

$$|u(x,t)| \le \frac{1}{\sqrt{4\pi t}} \left\|u_0\right\|_{L^1}. \tag{7}$$

This is the classical $t^{-1/2}$ dispersive estimate. The computation is clean, but it relies strongly on the phase being exactly quadratic. The next method uses only the local geometry of the phase and is therefore closer to what we need for the higher-order model.

3.4 Method 2: The cutoff argument

We now prove Proposition 3.1 by the cutoff method, which will also apply to the higher-order equation in Section 4. The argument follows the approach in [3, 2].

We treat (5) as an oscillatory integral with phase

$$\Phi(k) = -k^2 - \frac{x}{t}k. \tag{8}$$

Its derivatives are $\Phi'(k) = -2k - x/t$ and $\Phi''(k) = -2 \neq 0$. The unique stationary point of Φ is

$$k_0 = -\frac{x}{2t},$$

which is nondegenerate since $\Phi''(k_0) = -2 \neq 0$. Near k_0, the oscillation is slowest and the integrand contributes most. We split the integral at k_0 with radius $R > 0$:

$$u(x,t) = \frac{1}{\sqrt{2\pi}}(I_1 + I_2),$$

where

$$I_1 = \int_{|k-k_0|\le R} e^{-it\Phi(k)} \widehat{u_0}(k)\, dk, \qquad I_2 = \int_{|k-k_0|\ge R} e^{-it\Phi(k)} \widehat{u_0}(k)\, dk.$$

Estimate of I_1 (near part). Since the integration region has length $2R$,

$$|I_1| \le 2R \left\|\widehat{u_0}\right\|_{L^\infty}. \tag{9}$$

Estimate of I_2 (far part). On the region $|k-k_0| \ge R$, since $\Phi'(k) = -2(k-k_0)$ is linear and monotone, we have $|\Phi'(k)| \ge 2R > 0$. We use this to write the oscillating exponential as a derivative:

$$e^{-it\Phi(k)} = \frac{1}{-it\Phi'(k)}\, \partial_k\big(e^{-it\Phi(k)}\big),$$

and integrate by parts on each half-line $(-\infty, k_0 - R]$ and $[k_0 + R, \infty)$:

$$I_2 = \frac{1}{-it}\left[\frac{e^{-it\Phi(k)}\widehat{u_0}(k)}{\Phi'(k)}\right]_\partial + \frac{1}{it}\int_{|k-k_0|\ge R} e^{-it\Phi(k)}\, \partial_k\left(\frac{\widehat{u_0}(k)}{\Phi'(k)}\right) dk,$$

where $[\cdot]_\partial$ denotes the boundary terms at $k = k_0 \pm R$.

Boundary terms. At $k = k_0 \pm R$ we have $|\Phi'(k)| = 2R$, so

$$\left| \left[\frac{e^{-it\Phi(k)}\widehat{u_0}(k)}{\Phi'(k)} \right]_\partial \right| \leq \frac{2\, \|\widehat{u_0}\|_{L^\infty}}{2R} = \frac{\|\widehat{u_0}\|_{L^\infty}}{R}.$$

This contributes $\frac{1}{tR}\, \|\widehat{u_0}\|_{L^\infty}$ to $|I_2|$.

Interior integral. Applying the quotient rule:

$$\partial_k \left(\frac{\widehat{u_0}(k)}{\Phi'(k)} \right) = \frac{\partial_k \widehat{u_0}(k)}{\Phi'(k)} - \frac{\widehat{u_0}(k)\, \Phi''(k)}{(\Phi'(k))^2}.$$

On the far region, $\Phi'(k) = -2(k - k_0)$ and $\Phi''(k) = -2$, so $|\Phi'(k)| = 2\,|k - k_0| \geq 2R$ and $|\Phi''(k)| = 2$. Thus:

$$\frac{1}{|\Phi'(k)|} = \frac{1}{2\,|k - k_0|}, \qquad \frac{|\Phi''(k)|}{|\Phi'(k)|^2} = \frac{2}{4(k - k_0)^2} = \frac{1}{2(k - k_0)^2}.$$

Integrating each term over $|k - k_0| \geq R$:

$$\int_{|k-k_0|\geq R} \frac{|\partial_k \widehat{u_0}(k)|}{|\Phi'(k)|}\, dk \leq \frac{1}{2R}\, \|\partial_k \widehat{u_0}\|_{L^1}\,,$$

$$\int_{|k-k_0|\geq R} \frac{|\widehat{u_0}(k)|\, |\Phi''(k)|}{|\Phi'(k)|^2}\, dk \leq \frac{\|\widehat{u_0}\|_{L^\infty}}{2} \int_{|k-k_0|\geq R} \frac{dk}{(k - k_0)^2} = \frac{\|\widehat{u_0}\|_{L^\infty}}{R}.$$

Here it is important to use the L^∞ bound on $\widehat{u_0}$; estimating this term by $\|\widehat{u_0}\|_{L^1}$ would give the weaker factor R^{-2}. Combining all contributions:

$$|I_2| \lesssim \frac{1}{tR}\big(\|\widehat{u_0}\|_{L^\infty} + \|\partial_k \widehat{u_0}\|_{L^1}\big). \tag{10}$$

Balancing. Let $C_0 = \|\widehat{u_0}\|_{L^\infty} + \|\partial_k \widehat{u_0}\|_{L^1}$. Adding (9) and (10):

$$|u(x,t)| \lesssim R\, \|\widehat{u_0}\|_{L^\infty} + \frac{C_0}{tR}.$$

Setting $R \sim (tR)^{-1}$, i.e. $R^2 \sim t^{-1}$, gives $R \sim t^{-1/2}$. Substituting:

$$|u(x,t)| \lesssim t^{-1/2} C_0, \tag{11}$$

which is the conclusion of Proposition 3.1. The rate $t^{-1/2}$ arises because $|\Phi'(k)| \geq 2R$ on the far region: the lower bound is *linear* in R, reflecting the fact that k_0 is a nondegenerate stationary point and Φ' vanishes to first order there.

4 The Higher-Order Equation: No Stationary Points

4.1 Problem statement

We study the Cauchy problem for the third-order dispersive equation

$$iu_t = u_{xx} - iu_{xxx}, \qquad u(x,0) = u_0(x), \qquad x \in \mathbb{R},\ t > 0, \tag{12}$$

under the same assumptions (4) on u_0 as before. The main result of this section is:

Proposition 4.1. *Let u be the solution of* (12) *with initial data satisfying* (4)*. If $x/t > 1/3$, then for all $t > 0$,*

$$|u(x,t)| \lesssim t^{-1/3}\big(\|\widehat{u_0}\|_{L^\infty} + \|\partial_k \widehat{u_0}\|_{L^1}\big).$$

The regime $x/t > 1/3$ is where the phase has no stationary points, as we show below. The estimate below is a uniform worst-case bound in this regime, including the transition zone where x/t is close to $1/3$. The slower $t^{-1/3}$ rate compared to the Schrödinger $t^{-1/2}$ reflects the flatter quadratic geometry of the phase derivative near its minimum.

4.2 Fourier representation

We now consider the equation $iu_t = u_{xx} - iu_{xxx}$. Computing the Fourier transform: $\widehat{u_{xx}} = -k^2\widehat{u}$ and $\widehat{-iu_{xxx}} = -i(ik)^3\widehat{u} = k^3\widehat{u}$, so

$$\partial_t\widehat{u}(k,t) = i(k^3 - k^2)\widehat{u}(k,t).$$

Solving and inverting:

$$u(x,t) = \frac{1}{\sqrt{2\pi}}\int_{\mathbb{R}} e^{i(kx+t(k^3-k^2))}\widehat{u_0}(k)\,dk = \frac{1}{\sqrt{2\pi}}\int_{\mathbb{R}} e^{-it\Phi(k)}\widehat{u_0}(k)\,dk, \tag{13}$$

with phase function

$$\Phi(k) = k^2 - k^3 - \frac{x}{t}k. \tag{14}$$

The dispersion relation is $\omega(k) = k^3 - k^2$, and the group velocity is $\omega'(k) = 3k^2 - 2k$. The inflection point of ω, where $\omega''(k) = 6k - 2 = 0$, occurs at $k_* = 1/3$.

4.3 The no-stationary-point regime

The derivatives of Φ are

$$\Phi'(k) = 2k - 3k^2 - \frac{x}{t}, \qquad \Phi''(k) = 2 - 6k. \tag{15}$$

The stationary points of Φ satisfy $\Phi'(k) = -3k^2 + 2k - x/t = 0$, with discriminant $\Delta = 4 - 12\,x/t$. When

$$\frac{x}{t} > \frac{1}{3}, \tag{16}$$

we have $\Delta < 0$. Since the coefficient of k^2 in Φ' is $-3 < 0$, the quadratic $\Phi'(k)$ is everywhere negative:

$$\Phi'(k) < 0 \qquad \text{for all } k \in \mathbb{R}. \tag{17}$$

There are no stationary points.

4.4 Lower bound on $|\Phi'|$

Since $-\Phi'(k) = 3k^2 - 2k + x/t$ is a positive-definite quadratic, its minimum is achieved at $k_* = 1/3$:

$$\min_{k\in\mathbb{R}}(-\Phi'(k)) = -\Phi'(k_*) = \frac{1}{3} - \frac{2}{3} + \frac{x}{t} = \frac{x}{t} - \frac{1}{3} =: \delta.$$

Writing $-\Phi'(k) = 3(k-k_*)^2 + \delta$, we obtain

$$|\Phi'(k)| = 3(k-k_*)^2 + \delta \geq \delta > 0 \qquad \text{for all } k \in \mathbb{R}, \tag{18}$$

and on the far region $|k - k_*| \geq R$:

$$|\Phi'(k)| \geq 3R^2 + \delta. \tag{19}$$

4.5 Main estimate

Proposition 4.2. *Suppose $\widehat{u_0} \in L^\infty(\mathbb{R})$ and $\partial_k\widehat{u_0} \in L^1(\mathbb{R})$. If $x/t > 1/3$, then the solution of the equation $iu_t = u_{xx} - iu_{xxx}$ satisfies*

$$|u(x,t)| \lesssim t^{-1/3}\big(\|\widehat{u_0}\|_{L^\infty} + \|\partial_k\widehat{u_0}\|_{L^1}\big).$$

Proof. Fix $R > 0$ and $k_* = 1/3$. Split the integral as

$$u(x,t) = \frac{1}{\sqrt{2\pi}}(I_{\text{near}} + I_{\text{far}}),$$

where near and far regions are $|k - k_*| \leq R$ and $|k - k_*| \geq R$.

Near part.

$$|I_{\text{near}}| \le 2R\,\|\widehat{u_0}\|_{L^\infty}\,. \tag{20}$$

Far part. On the far region, (19) gives $|\Phi'(k)| \ge 3R^2$. Since $\Phi' < 0$ is monotone on each half-line $(-\infty, k_*]$ and $[k_*, \infty)$, write $e^{-it\Phi(k)} = \frac{1}{-it\Phi'(k)}\,\partial_k(e^{-it\Phi(k)})$ and integrate by parts on each piece:

$$I_{\text{far}} = \frac{1}{it}\int_{|k-k_*|\ge R} e^{-it\Phi(k)}\,\partial_k\left(\frac{\widehat{u_0}(k)}{\Phi'(k)}\right) dk + B_R,$$

where B_R collects boundary terms at $k = k_* \pm R$.

Boundary terms. Since $|\Phi'(k_* \pm R)| \ge 3R^2$:

$$|B_R| \lesssim \frac{\|\widehat{u_0}\|_{L^\infty}}{tR^2}.$$

Interior integral. By the quotient rule,

$$\partial_k\left(\frac{\widehat{u_0}}{\Phi'}\right) = \frac{\partial_k\widehat{u_0}}{\Phi'} - \frac{\widehat{u_0}\,\Phi''}{(\Phi')^2}.$$

On the far region, $|\Phi'(k)| \ge 3(k-k_*)^2$ and $|\Phi''(k)| = 6\,|k-k_*|$, so

$$\frac{1}{|\Phi'(k)|} \lesssim \frac{1}{(k-k_*)^2}, \qquad \frac{|\Phi''(k)|}{|\Phi'(k)|^2} = \frac{6\,|k-k_*|}{9(k-k_*)^4} = \frac{2}{3(k-k_*)^3} \le \frac{2}{3R^2\,|k-k_*|}.$$

Using $1/(k-k_*)^2 \le 1/R^2$ for the first term and the integrability of $|k-k_*|^{-3}$ on the two far half-lines for the second term, we get

$$\int_{|k-k_*|\ge R}\left|\partial_k\left(\frac{\widehat{u_0}}{\Phi'}\right)\right| dk \lesssim \frac{1}{R^2}\,\|\partial_k\widehat{u_0}\|_{L^1} + \|\widehat{u_0}\|_{L^\infty}\int_{|k-k_*|\ge R}\frac{dk}{|k-k_*|^3} \lesssim \frac{1}{R^2}\big(\|\partial_k\widehat{u_0}\|_{L^1} + \|\widehat{u_0}\|_{L^\infty}\big).$$

Here again the second term is controlled by the L^∞ norm of $\widehat{u_0}$, not by its L^1 norm. Therefore

$$|I_{\text{far}}| \lesssim \frac{1}{tR^2}\big(\|\widehat{u_0}\|_{L^\infty} + \|\partial_k\widehat{u_0}\|_{L^1}\big). \tag{21}$$

Balancing. Adding (20) and (21) and setting $R \sim 1/(tR^2)$ gives $R^3 \sim t^{-1}$, hence $R \sim t^{-1/3}$. Substituting:

$$|u(x,t)| \lesssim t^{-1/3}\big(\|\widehat{u_0}\|_{L^\infty} + \|\partial_k\widehat{u_0}\|_{L^1}\big). \qquad \square$$

4.6 Comparison with the Schrödinger case

The mechanism behind the $t^{-1/3}$ rate is identical to that of a degenerate stationary point: on the far region $|k-k_*| \ge R$, the lower bound $|\Phi'(k)| \ge 3R^2$ is quadratic in R. This is because $k_* = 1/3$ is the point where $|\Phi'|$ attains its minimum. When x/t is close to $1/3$, we have $|\Phi'(k)| = 3(k-k_*)^2 + \delta$ with small $\delta = x/t - 1/3 > 0$, so the worst-case geometry is essentially quadratic near k_*. The same quadratic vanishing that produces the $t^{-1/3}$ rate in the degenerate stationary-point problem therefore drives the balancing here as well.

For the free Schrödinger equation, the lower bound on the far region is $|\Phi'(k)| \ge 2R$, linear in R, because Φ' vanishes only to first order at the stationary point. This gives balance $R \sim t^{-1/2}$ and decay $t^{-1/2}$. The quadratic lower bound $3R^2$ in the present case produces the slower $t^{-1/3}$ rate, reflecting the flatter geometry of Φ' near its minimum.

5 Numerical Simulations

5.1 Numerical method

Each frame of the simulation computes: FFT → rotate each mode → IFFT. Both PDEs are linear with constant coefficients, so the Fourier transform fully diagonalizes them. After transforming, each Fourier mode $\widehat{u}(k)$ satisfies its own independent ODE:

$$\text{Higher-order:} \quad \partial_t \widehat{u} = i(k^2 - k^3)\,\widehat{u},$$
$$\text{Schrödinger:} \quad \partial_t \widehat{u} = ik^2\,\widehat{u}.$$

Both have the form $\partial_t \widehat{u} = i\lambda(k)\,\widehat{u}$, whose exact solution is

$$\widehat{u}(k,\,t) = \widehat{u}(k,\,0) \cdot e^{i\lambda(k)t}.$$

Since $\lambda(k)$ is real, $e^{i\lambda\,dt}$ has modulus 1 — it is a pure rotation in $\mathbb{C}$, applied as multiplication by $\cos(\lambda\,dt) + i\sin(\lambda\,dt)$. This means there is *no time-stepping approximation at all.* The integrator is exact for the linear PDE — no CFL condition, no stability constraint, no truncation error in dt. The only numerical error comes from FFT rounding, of order $\sim 10^{-15}$, which is why $\|u\|_{L^2}$ stays conserved to machine precision throughout the simulation. The limitation is that this only works for linear, constant-coefficient equations.

5.2 Simulations

We simulate both equations with Gaussian initial data $u_0(x) = e^{-x^2/2}$, so $\|u_0\|_{L^\infty} = 1$. Figure 2 shows $\|u(\cdot,t)\|_{L^\infty}$ over time for both equations, together with the reference curves $c_1 t^{-1/3}$ and $c_2 t^{-1/2}$.

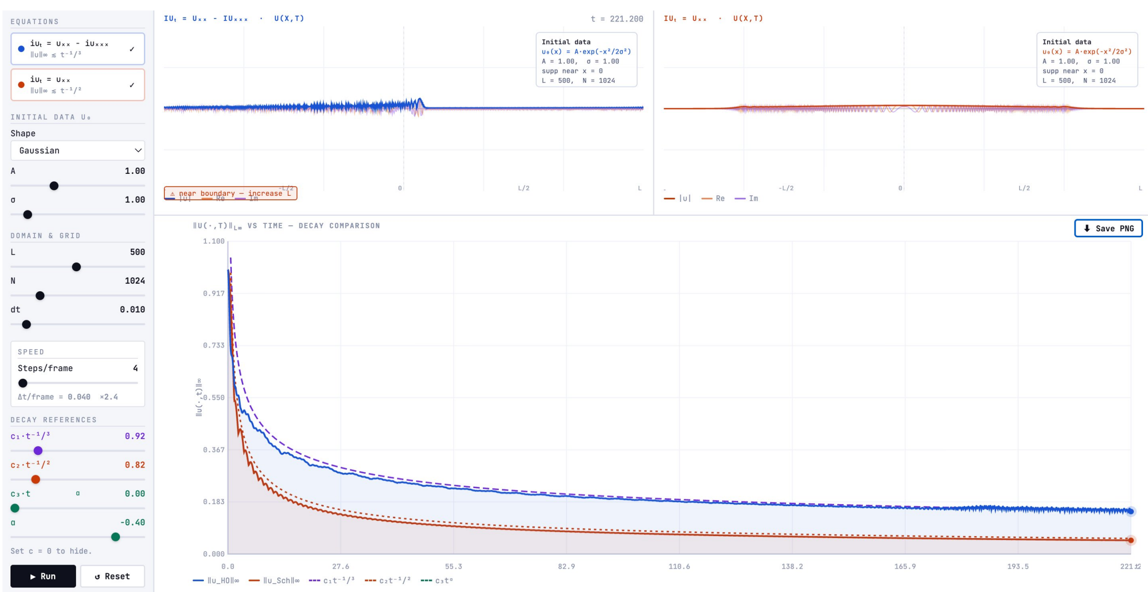

Figure 2: $\|u(\cdot,t)\|_{L^\infty}$ vs. time for the higher-order equation $iu_t = u_{xx} - iu_{xxx}$ (blue) and the free Schrödinger equation $iu_t = u_{xx}$ (red), with fitted reference curves $c_1 t^{-1/3}$ and $c_2 t^{-1/2}$ (dashed). Both decay rates match the theoretical predictions closely, with constants $c_1 \approx 0.92$ and $c_2 \approx 0.82$ comparable to the initial supremum $\|u_0\|_{L^\infty} = 1$.

The fitted constants $c_1 \approx 0.92$ and $c_2 \approx 0.82$ are both of order one, comparable to the initial $\|u_0\|_{L^\infty} = 1$. This confirms that the theoretical estimates $\|u(\cdot,t)\|_{L^\infty} \lesssim t^{-1/2}$ and $\|u(\cdot,t)\|_{L^\infty} \lesssim t^{-1/3}$ are sharp in the sense that the implicit constant cannot be taken much smaller than the initial amplitude.

6 Conclusion

The goal of this paper was to estimate the L^∞ decay rate for two dispersive equations. For the free Schrödinger equation $iu_t = u_{xx}$ we proved $\|u(\cdot,t)\|_{L^\infty} \lesssim t^{-1/2}$, and for the third-order model $iu_t = u_{xx} - iu_{xxx}$ we proved the uniform worst-case bound $\|u(\cdot,t)\|_{L^\infty} \lesssim t^{-1/3}$ in the regime $x/t > 1/3$. Both estimates require regularity assumptions on the initial data; in particular the cutoff argument relies on $\partial_k \widehat{u_0} \in L^1$, which limits the class of admissible initial data. The numerical simulations confirm that both decay rates are achieved in practice, with fitted constants of order one relative to the initial amplitude, indicating that the estimates are sharp.

References

[1] L. C. Evans, *Partial Differential Equations*, 2nd ed., Graduate Studies in Mathematics, vol. 19, American Mathematical Society, Providence, RI, 2010.

[2] P. Germain, F. Pusateri, and F. Rousset, The nonlinear Schrödinger equation with a potential, *arXiv:1704.00061*, 2017.

[3] *An Introduction to Dispersive Equations*, Lecture Notes, Michigan State University.